A novel mouse strain optimized for chronic human antibody administration

Aaron Gupta[a,1], Patrick Smith[a,1], Stylianos Bournazos[a], and Jeffrey V. Ravetch[a,2]

[a]Laboratory of Molecular Genetics & Immunology, The Rockefeller University, New York, NY 10065

Contributed by Jeffrey V. Ravetch; received December 20, 2021; accepted February 2, 2022; reviewed by Tomohiro Kurosaki and Diane Mathis

Therapeutic human IgG antibodies are routinely tested in mouse models of oncologic, infectious, and autoimmune diseases. However, assessing the efficacy and safety of long-term administration of these agents has been limited by endogenous anti-human IgG immune responses that act to clear human IgG from serum and relevant tissues, thereby reducing their efficacy and contributing to immune complex–mediated pathologies, confounding evaluation of potential toxicity. For this reason, human antibody treatment in mice is generally limited in duration and dosing, thus failing to recapitulate the potential clinical applications of these therapeutics. Here, we report the development of a mouse model that is tolerant of chronic human antibody administration. This model combines both a human IgG1 heavy chain knock-in and a full recapitulation of human Fc receptor (FcγR) expression, providing a unique platform for in vivo testing of human monoclonal antibodies with relevant receptors beyond the short term. Compared to controls, hIgG1 knock-in mice mount minimal anti-human IgG responses, allowing for the persistence of therapeutically active circulating human IgG even in the late stages of treatment in chronic models of immune thrombocytopenic purpura and metastatic melanoma.

immunoglobulin | tolerance | Fc receptors | humanized mouse

In vivo assessment of the therapeutic and adverse effects of human antibodies in mouse model systems has long been confounded by intolerance for these agents. Administration of human immunoglobulins to mice inevitably results in mouse anti-human IgG responses, likely due to foreign epitopes present in human IgG proteins. Previous studies have shown that these responses develop within days to weeks of IgG administration and serve to enhance clearance of human IgG (1, 2), interfere with antigen binding and effector function, and diminish therapeutic activity (3), while also potentially contributing pathological sequalae of immune complex deposition (4). For this reason, murine studies of human antibody treatment in our laboratory and others have been limited to the short term (approximately 2 wk) to ensure that anti-human IgG responses are not confounding meaningful results that may apply to patients (5–7).

Prior studies have only partially characterized this response and have reported inconsistent results. For instance, some studies argue that the route of immunization (i.e., intravenous vs. intraperitoneal vs. intradermal) may play a role in eliciting an anti-human response (3), although the results are inconsistent. It also has been suggested that IgG1 is the dominant mouse subclass that responds to exogenous human IgG, although there are substantial mouse IgG2b and IgG2c anti-IgG titers that contribute as well (4). Further, one study indicated that, in order for a mouse anti-human IgG response to develop, the cognate antigen of the administered human antibody must be present in the mouse model (1), implying that immune complexes, not monomeric antibodies, initiate these responses. Finally, the kinetics of this response are unclear; some studies suggest it requires up to 9 wk for a significant anti-human response to develop (8), while others count less than 1 wk (1). Despite these characterizations, no study, to date, has provided a robust solution to this intolerance, which continues to limit the extent of in-depth studies of antibody efficacy and safety.

In this study, we present a mouse model that is appropriate for the study of long-term, repeated administration of human antibodies. Tolerance to human IgG is conferred by germline knock-in of the human IgG1 (hIgG1) heavy chain (*IGHG1*) in place of mouse *Ighg2c*. In addition, this knock-in has been combined with a previously described model of human FcγR expression and function (9), so that the relevant effector functions of these exogenous human antibodies can be investigated. In the knock-in mouse, hIgG1 pairs appropriately with mouse light chains, is expressed on the surface of B cells, and is elicited by immunization to both thymic-dependent (T-dependent) and thymic-independent (T-independent) antigens. Knock-in mice are tolerant of repeated administration of human IgG through multiple routes of immunization, and therefore allow for the in vivo characterization of antibody-mediated responses in the long term.

Results

Knock-In of hIgG1 into the Mouse Ig Heavy Chain Locus. The hIgG1 was knocked in by precise replacement of the native mouse *Ighg2c* coding sequence with human *IGHG1* via CRISPR-Cas9 gene editing of C57BL/6J embryonic stem (ES) cells (Fig. 1). In addition to this sequence, an FRT-loxP-

Significance

Species differences in IgG Fc–Fcγ receptor (FcγR) interactions have made humanized mouse models an attractive strategy to evaluate the efficacy and toxicity of human antibodies. We previously published a humanized FcγR mouse model that fully recapitulates the expression and function of these receptors in vivo. However, the immunogenicity of exogenous human IgG has made long-term assessment of antibody function challenging, since endogenous mouse anti-human IgG responses limit the duration and success of these studies. Here, we present a mouse strain that expresses human IgG1 and FcγRs, thereby conferring tolerance to chronic administration of human IgG and enabling functional assessment of antibodies. Because this strain is appropriate for chronic disease models, we expect that researchers will benefit from its use.

Author contributions: A.G., S.B., and J.V.R. designed research; A.G. and P.S. performed research; P.S. contributed new reagents/analytic tools; A.G. analyzed data; and A.G., S.B., and J.V.R. wrote the paper.

Reviewers: T.K., Immunology Frontier Research Center, Osaka University; and D.M., Harvard Medical School.

The authors declare no competing interest.

[1]A.G. and P.S. contributed equally to this work.

[2]To whom correspondence may be addressed. Email: ravetch@rockefeller.edu.

This article contains supporting information online at http://www.pnas.org/lookup/suppl/doi:10.1073/pnas.2123002119/-/DCSupplemental.

Published March 2, 2022.

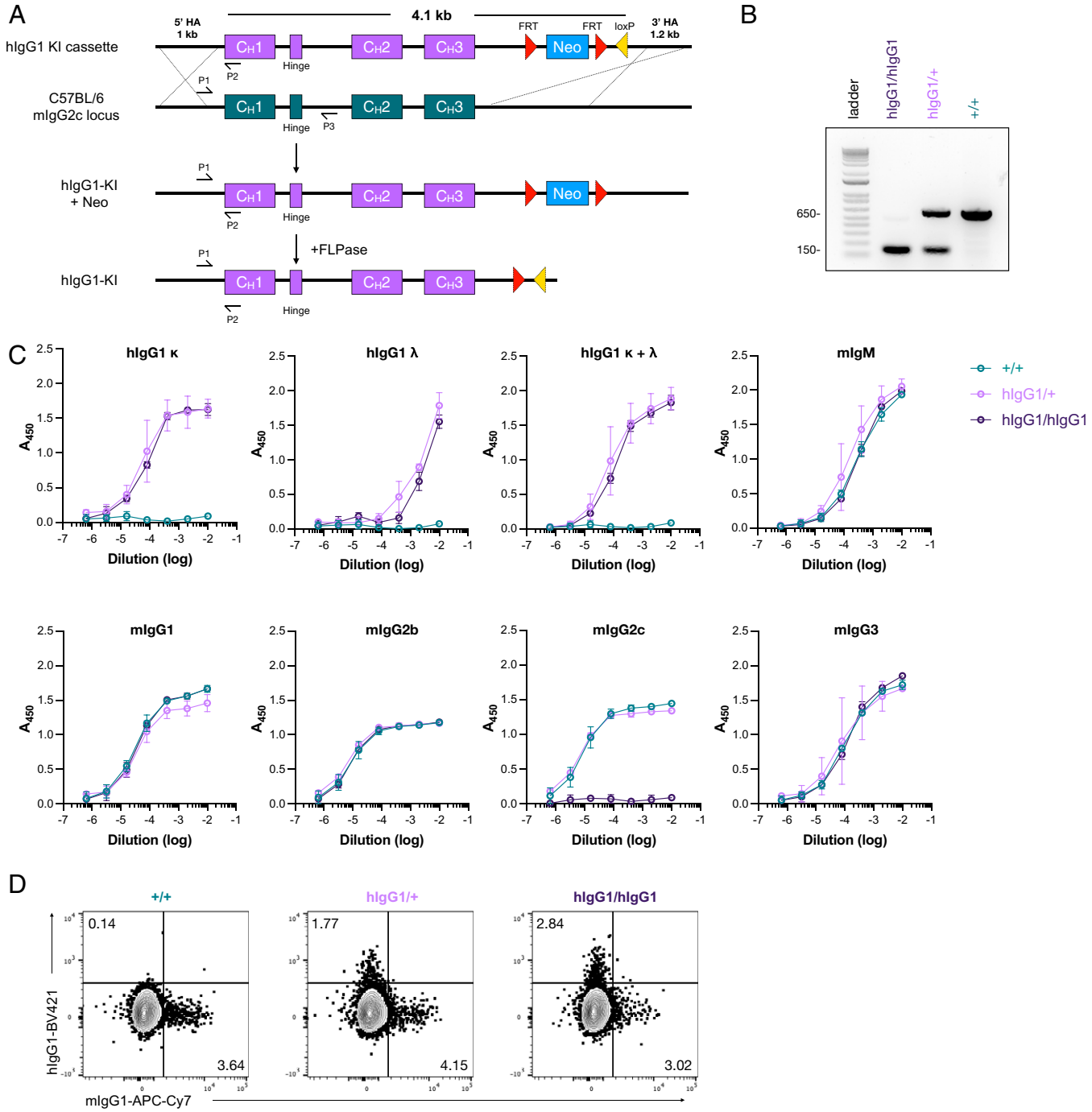

Fig. 1. Generation and characterization of hIgG1 knock-in mouse. (*A*) Targeting the mouse IgG2c heavy chain locus for replacement with a construct bearing the hIgG1 heavy chain and FRT-loxP-Neomycin cassette. Red triangles represent FRT sites, and the yellow triangle represents a loxP site. (*B*) Representative ($n = 5$ each strain) genotyping PCR of hIgG1/hIgG1, hIgG1/+, and $^{+/+}$ mice. (*C*) Serum IgG titers in $^{+/+}$, hIgG1/+, and hIgG1/hIgG1 mice on human FcγR background measured by ELISA. Anti-lambda and anti-kappa light chain antibodies were used for capture, and HRP-conjugated isotype-specific antibodies were used for detection. Data are displayed as mean ± SEM ($n = 3$). (*D*) Representative ($n = 3$) flow cytometry analysis of IgG surface expression on splenic B220+ cells.

neomycin cassette was appended to the 3′ end of the targeting cassette to select properly edited ES cells, as well as 5′ and 3′ homology arms flanking the insert to assist with homology-directed repair (HDR) (Fig. 1*A*). This strategy preserved upstream and downstream switch and regulatory regions, with the intent that hIgG1 would mimic the expression profile of mouse IgG2c, and that other mouse subclasses were undisturbed. Mouse IgG2c was specifically targeted since it most closely approximates the FcγR-binding profile of hIgG1. Mice positive for the knock-in allele were screened using a common forward primer and reverse primers specific for either mIgG2c or hIgG1 (Fig. 1*B*). Serum analysis of heterozygotes (hIgG1/+) and homozygotes (hIgG1/hIgG1) demonstrates pairing of hIgG1 heavy chain with mouse kappa and lambda light chains and successful replacement of the mIgG2c heavy chain (Fig. 1*C*). As expected, the knock-in has normal endogenous mouse

IgG levels as compared to C57BL6/J mice. Flow cytometry analysis of B-lineage cells in the spleen shows the knock-in preserves normal B cell development (*SI Appendix*, Fig. S2). Indeed, analysis of B220^{+} splenic B cells from knock-in mice shows robust surface expression of hIgG1, indicating pairing of membrane-bound hIgG1 with B cell receptor (BCR) components is intact (Fig. 1*D*). These mice develop normally, are fertile, and have no evidence of spontaneous pathology under the specific pathogen-free conditions maintained in the Rockefeller University animal facility.

hIgG1 Knock-In Mice Mount Normal Humoral Responses. To determine whether knock-in mice mount hIgG1 responses to specific immunization, wild-type or heterozygote knock-in mice were immunized with the model haptenated antigen, 4-hydroxy-3-nitrophenylacetyl (NP). T-independent responses were measured by a single immunization with NP-Ficoll adjuvanted with Complete Freund's Adjuvant. After 2 wk, anti-NP hIgG1 titers were detected, and persisted until the end of the study at 4 wk (Fig. 2*A*). Similarly, T-dependent immunization with NP-ovalbumin in a prime–boost dosing schedule 2 wk apart induced a strong NP-specific hIgG1 response in the knock-in mice (Fig. 2*B*). The subclass composition of endogenous mouse IgG responses to NP were consistent with previous reports of T-independent and T-dependent immunization (*SI Appendix*, Figs. S3 and S4) (10, 11). These studies confirm that hIgG1 can participate in processes of affinity maturation and class switch recombination in response to immunization.

hIgG1 Knock-In Tolerizes Mice to Chronic Human Antibody Administration. Previous studies have demonstrated that repeated dosing of human antibodies induces a strong mouse anti-human response which leads to rapid clearance of human IgG and loss of activity (1, 3, 4, 8). We hypothesized that native expression of hIgG1 would endow knock-in mice with tolerance to exogenous hIgG1. To investigate the issue of antibody clearance, wild-type C57BL6/J or hIgG1 knock-in mice were dosed weekly with 100 μg of the fully human HIV anti-gp120 monoclonal, 3BNC117-hIgG1 (Fig. 3*A*) (12). After five cycles of treatment (day 35), knock-in mice were able to maintain high serum levels of 3BNC117, while controls rapidly cleared the antibody to levels at or below the limit of detection of the assay (Fig. 3*B*). We presumed the rapid clearance was due to a strong mouse anti-human IgG1 response that was absent in the knock-in mice, since clearance accelerated considerably after 2 wk to 3 wk of administration. To test this hypothesis, we immunized knock-in and control mice weekly with 2B8-hIgG1, an anti-CD20 clone with human framework regions, but mouse complementarity-determining regions (Fig. 3*C*). Weekly intravenous administration of 2B8-hIgG1 resulted in mouse anti-human IgG1 titers detectable in control mice by week 3. By week 5, high titers were evident in control mice, while knock-ins had significantly lower levels of mouse anti-hIgG1 antibodies (Fig. 3*D*). Unexpectedly, similar experiments with other human subclasses of IgG routinely used in clinical studies (IgG2 and IgG4) demonstrated that the knock-in mouse is tolerant of 2B8-hIgG4 compared to controls, while 2B8-IgG2 was not strongly immunogenic in either mouse (*SI Appendix*, Fig. S5). Tolerance to IgG4 may be due to its ∼90% sequence identity with hIgG1, versus ∼62% with mouse IgG1 heavy chain. Notably, none of the mice immunized with hIgG1 antibodies mounted a significant response to the constant region of the human kappa light chain, as shown by sandwich enzyme-linked immunosorbent assay (ELISA) using an irrelevant mouse IgG1-human kappa chimeric antibody as capture (Fig. 3*E*).

hIgG1 Knock-In Mice in a Chronic Model of Immune Thrombocytopenia Purpura. Exogenous human antibodies are often used to induce pathology in mouse models of autoimmune diseases, but their efficacy over time is limited by mouse anti-human responses to those antibodies (4). One common model to induce immune thrombocytopenic purpura (ITP) in mice uses the antiplatelet IIb glycoprotein antibody, 6A6, which, when administered intravenously (i.v.), targets platelets for clearance by macrophages (13, 14). Because the mechanism of platelet

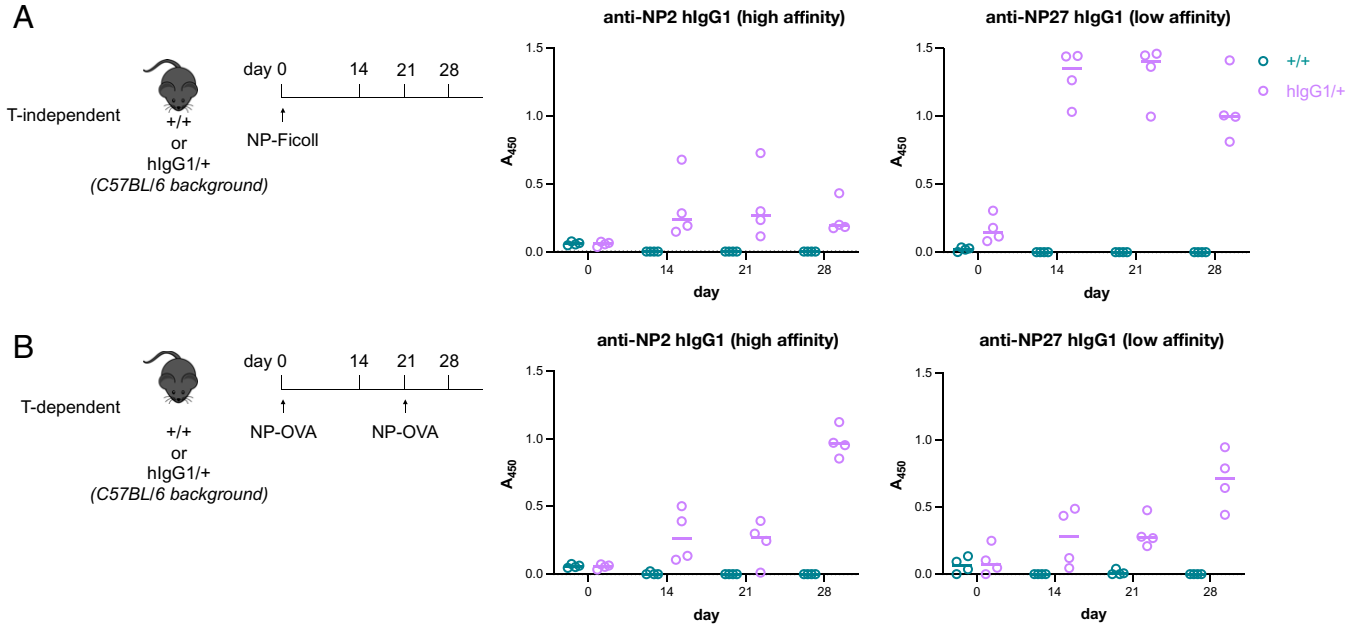

Fig. 2. The hIgG1 knock-in mouse has normal B-lineage development and shows robust antigen-specific hIgG1 response to immunization. (*A*) T-independent intraperitoneal immunization of mice with the indicated genotypes with 50 μg of NP54-Ficoll in alum. Serum was harvested at the indicated time points and analyzed for NP-specific IgG by ELISA. (*B*) T-dependent intraperitoneal immunization of mice with the indicated genotypes with 50 μg of NP17-OVA in alum. Mice were subsequently boosted with 50 μg of NP17-OVA on day 21. Serum was harvested at the indicated time points and analyzed for NP-specific IgG by ELISA. Data are displayed as individual biological replicates with a line representing the mean (n = 4 each strain).

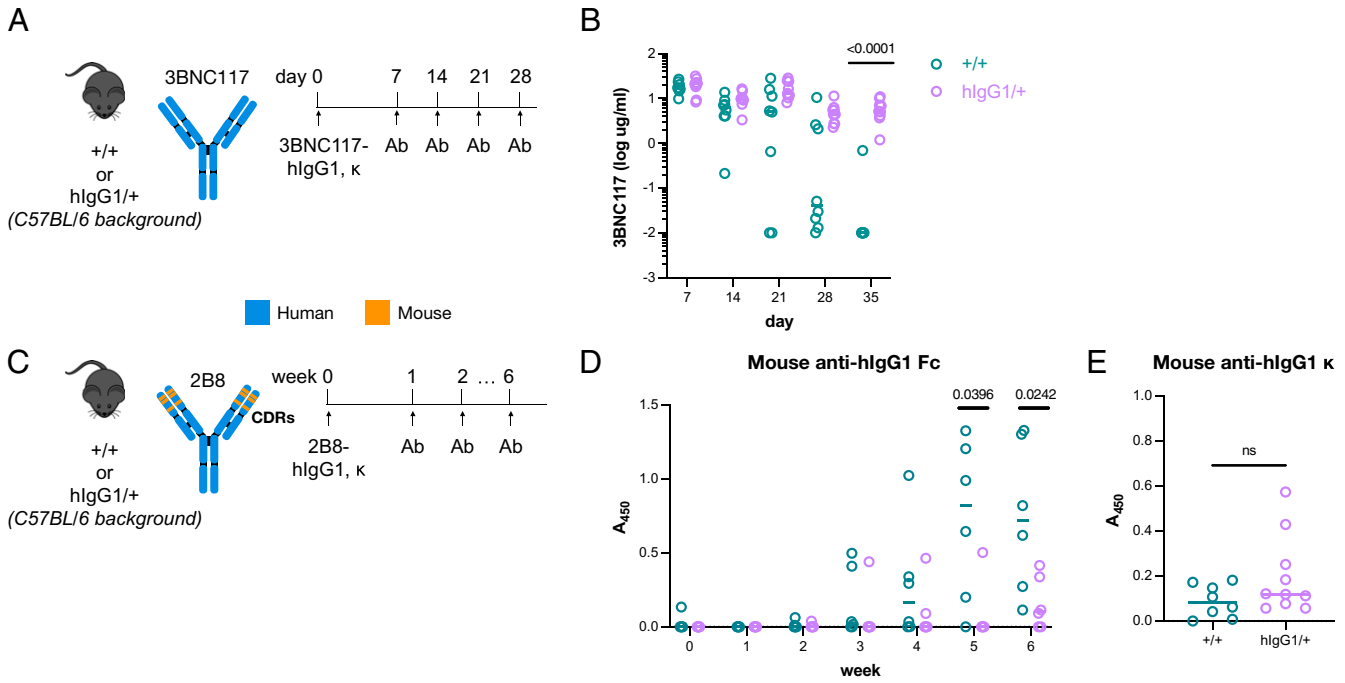

Fig. 3. The hIgG1 knock-in tolerizes mice to chronic human antibody administration. (*A* and *B*) Mice of the indicated genotypes were repeatedly administered 100 μg of 3BNC117-hIgG1 i.p. on the days indicated. Serum levels of 3BNC117-hIgG1 were measured by ELISA using recombinant gp120 for capture and using anti–hIgG-HRP for detection. Data are shown as individual biological replicates, with a horizontal line representing the mean ($n = 8$ each strain). (*C* and *D*) Mice of the indicated genotypes were administered 100 μg of 2B8-hIgG1 i.p. each week for 6 wk. Mouse anti-hIgG1 Fc titers were measured by ELISA using hIgG1 Fc for capture and using anti-mouse IgG-HRP for detection. Data are shown as individual biological replicates, with a horizontal line representing the mean ($n = 6$ each strain). (*E*) Mouse anti-human kappa constant region titers were measured by ELISA using an irrelevant mouse IgG1-human kappa chimeric antibody as capture and using anti-human Fc-HRP for detection. Data are shown as individual biological replicates with a horizontal line representing the mean ($n = 8$ to 10 each strain).

clearance in this model relies on Fc–FcγR interactions, it was necessary to cross the hIgG1 knock-in mice with a mouse strain that is fully humanized for FcγRs. To approximate a chronic version of this ITP model (15), mice bearing the knock-in allele and human FcγRs were administered 6A6-hIgG1 for three consecutive days and then allowed to recover for 4 d, over which time their platelets recovered to normal levels (Fig. 4*A*). Platelet counts were measured on each day. This treatment schedule was repeated twice, for a total of three cycles. In the first two cycles, differences in 6A6-hIgG1 platelet depletion between the two strains were insignificant. In the third cycle, only mice bearing the hIgG1 knock-in allele were able to deplete platelets efficiently (Fig. 4*C*). This difference was accompanied by high mouse anti-hIgG1 Fc titers in control mice, which presumably led to enhanced clearance of 6A6-hIgG1 and therefore interfered with its platelet depleting activity (Fig. 4*B*). This ITP model demonstrates the utility of a mouse that is tolerant of human antibody administration and can therefore recapitulate the pathology of an autoimmune disease in a chronic setting.

hIgG1 Knock-In Mice Show Improved Clinical Outcomes in a B16-F10 Melanoma Chronic Treatment Model. Human antibody treatment in mouse models of cancer is limited to the short term by endogenous anti-human IgG responses that limit efficacy of these agents. This is evident from human antibody treatment schedules, which generally take place over a maximum of 2 wk. To demonstrate that antibody treatment in the knock-in mouse does not have such restrictions, we subjected the knock-in and control mice to a chronic treatment model of metastatic B16-F10 melanoma (16). Mice from each group were pretreated twice over 3 wk with TA99, an antibody clone with mouse variable and human constant regions that targets gp75 on the surface of B16 cells and has been shown to effectively prevent lung metastases in an Fc-dependent manner (17) (Fig. 5*A*). Because TA99 requires strong activating FcγR engagement for efficacy, an Fc optimized variant (GAALIE) of IgG1 was used, which exhibits an improved binding profile to human activating FcγRs (7, 18). As expected, pretreatment resulted in detectable mouse anti-hIgG1 Fc titers in control mice, but not in knock-in mice (Fig. 5*B*). Importantly, this study also demonstrates that expression of wild-type hIgG1 tolerizes these mice to an Fc-engineered variant that harbors three mutations in the Cγ2 region, showing the potential use of this model to quantify the immunogenicity of Fc variants. Following pretreatment, mice were i.v. injected with B16-F10 cells, and some groups were treated with four doses of TA99-hIgG1-GAALIE at the time points indicated. Two weeks after tumor inoculation, lungs were excised and analyzed for metastases. As expected, mice treated with phosphate-buffered saline (PBS) developed widespread metastases that gave their lungs a blackened appearance. Control mice that were intolerant of hIgG1 after 2 wk were only partially treated by TA99-hIgG1-GAALIE, while the lungs of knock-in mice were free of significant metastases (Fig. 5 *C* and *D*). Consistent with these results, TA99 could not be detected in the serum of control mice on Day 14, likely due to enhanced clearance by the formation of mouse anti-hIgG1 immune complexes, while levels persisted at therapeutic levels in most knock-in mice (Fig. 5*E*). Based on these studies, this knock-in mouse model, which is free of interfering endogenous anti-hIgG1 responses, provides a useful platform to study human antibody efficacy and toxicity in disease models that require long-term treatment.

Discussion

In the present study, we addressed the issue of chronic administration of human antibodies by developing a mouse model with

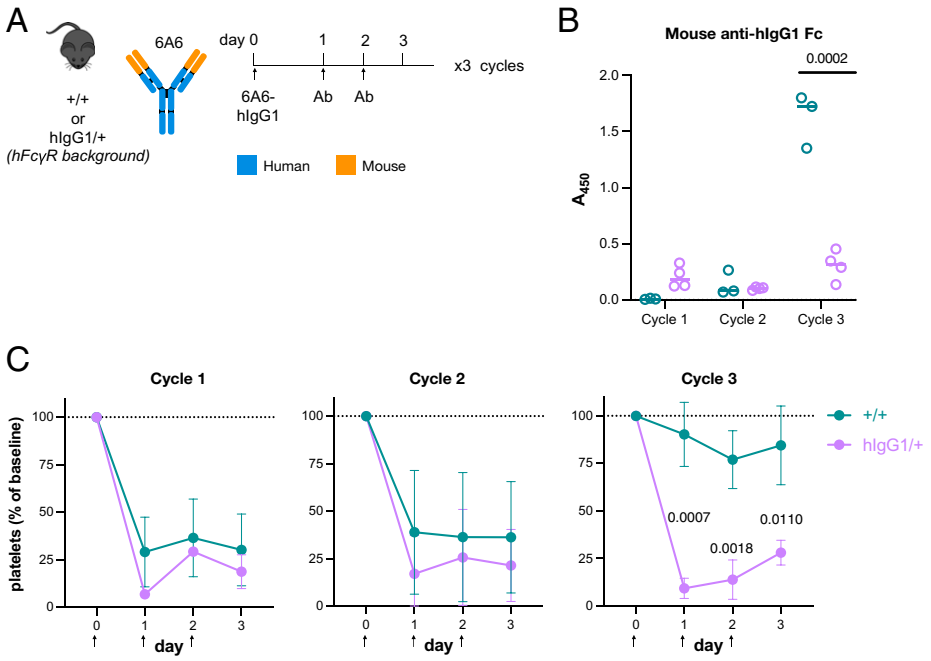

Fig. 4. The hIgG1 knock-in mice in a chronic model of ITP. (*A*) Mice of the indicated genotypes were repeatedly administered 10 μg of 6A6-hIgG1 intravenously three times per week for 3 wk. (*B*) Mouse anti-hIgG1 Fc titers were measured by ELISA using hIgG1 Fc for capture and using anti-mouse IgG-HRP for detection. Data are shown as individual biological replicates, with a horizontal line representing the mean (n = 3 to 4 each strain). (*C*) Platelet depletion during three cycles of 6A6-hIgG1 treatment. Platelet count is reported as a percentage of platelet count at the start of each cycle. Data are displayed as mean ± SEM (n = 3 to 4 each strain).

tolerance for these agents. By combining this knock-in with our previously published human FcγR model, we have created a system to extensively assess the specific activity and effector function of human antibodies regardless of treatment length or disease chronicity. Importantly, the hIgG1 heavy chain correctly pairs with endogenous mouse kappa and lambda light chains, is adequately expressed in its membrane form on the surface of B cells, and endows these mice with tolerance for exogenous human IgG. This newfound tolerance has major implications for the serum half-life of exogenous antibodies, and their ability to opsonize target cells, proteins, or virions and to perform essential effector functions via Fc–FcγR interactions. Fortunately, knock-in mice avoid the strong mouse anti-human IgG1 Fc response shown, in this study, to develop as early as 2 wk after first treatment. Based on the kinetics of this response and the coinciding decline in hIgG1 activity in models of chronic ITP and metastatic melanoma, it is likely that mouse anti-hIgG1 antibodies directly interfere with antibody effector function. This may be especially true in the models tested, which rely extensively on Fc–FcγR interactions. To our surprise, the 106-aa human kappa light chain constant region was not immunogenic to wild-type C57BL6/J mice, despite sharing only 60% sequence identity with its mouse homolog. Therefore, expression of hIgG1 Cγ1 through Cγ3 appears sufficient to confer tolerance to hIgG1.

Although there are previous reports of hIgG1 knock-ins (19, 20), tolerance of exogenous hIgG1 has never been characterized. Further, although some of these models combine expression of ligand (human IgG) with the full recapitulation of structure and function of their cognate receptors (human FcγRs), they do so on mixed genetic backgrounds, thereby making the present model a unique platform to precisely study human antibodies in mice without confounding factors. In particular, this model will best approximate disease contexts where long-term treatment with human IgG treatment is necessary, such as relapsing and remitting tumors, chronic autoimmune diseases, and chronic infections.

Although the current model presents considerable advantages over previous iterations in terms of human IgG tolerance, it is not well suited to answer questions about the role of Fc–FcγR interactions in the development of human antibody responses. This is due to species differences in isotype expression, BCR components, regulation of class switch recombination, and a host of other genetic factors that govern these responses. In addition, although the knock-in mice express endogenous hIgG1, it is at levels lower than in humans, in which it is the dominant subclass. Here, hIgG1 is regulated similarly to mouse IgG2c, a less abundant subclass in mice. Further, in mice and humans, endogenous serum IgG competes for receptor occupancy of the neonatal Fc receptor (FcRn), thereby setting the bounds for the half-life of antibodies, so expression of the human FcRn would be required to accurately recapitulate half-life in humans. Other improvements to the model include human versions of the type II FcRs CD23 and DC-SIGN (21–25).

In summary, we conclude that this mouse model is tolerant of human antibodies and will be a useful tool for researchers who wish to study human antibody treatment and pathology in the long term.

Materials and Methods

Generation of the hIgG1-KI Mouse. The hIgG1-KI mouse was designed to express the heavy chain of human *IGHG1* by direct replacement of the Cγ1 through Cγ3 region of mouse *Ighg2c*. The nascent human heavy chain peptide would then pair with both mouse kappa and lambda light chains to form a fully intact and functioning hIgG1 antibody.

Targeting Mouse Ighg2c in C57BL/6 Mice. The construct to target the mouse IgG2c heavy chain locus was generated by joining a 1-kb 5′ homology arm upstream of the mouse *Ighg2c* Cγ1 region, human *IGHG1* Cγ1 through Cγ3, and a 1.2-kb 3′ homology arm downstream of the mouse *Ighg2c* Cγ3 region. Homology arms were generated by PCR amplification (Pfu Turbo DNA Polymerase, Agilent Technologies) from C57BL/6 genomic DNA, and human *IGHG1* Cγ1 through Cγ3 were generated from PCR amplification of from a DNA library isolated from human blood (BAC clone RCPI-11-417P24, CHORI).

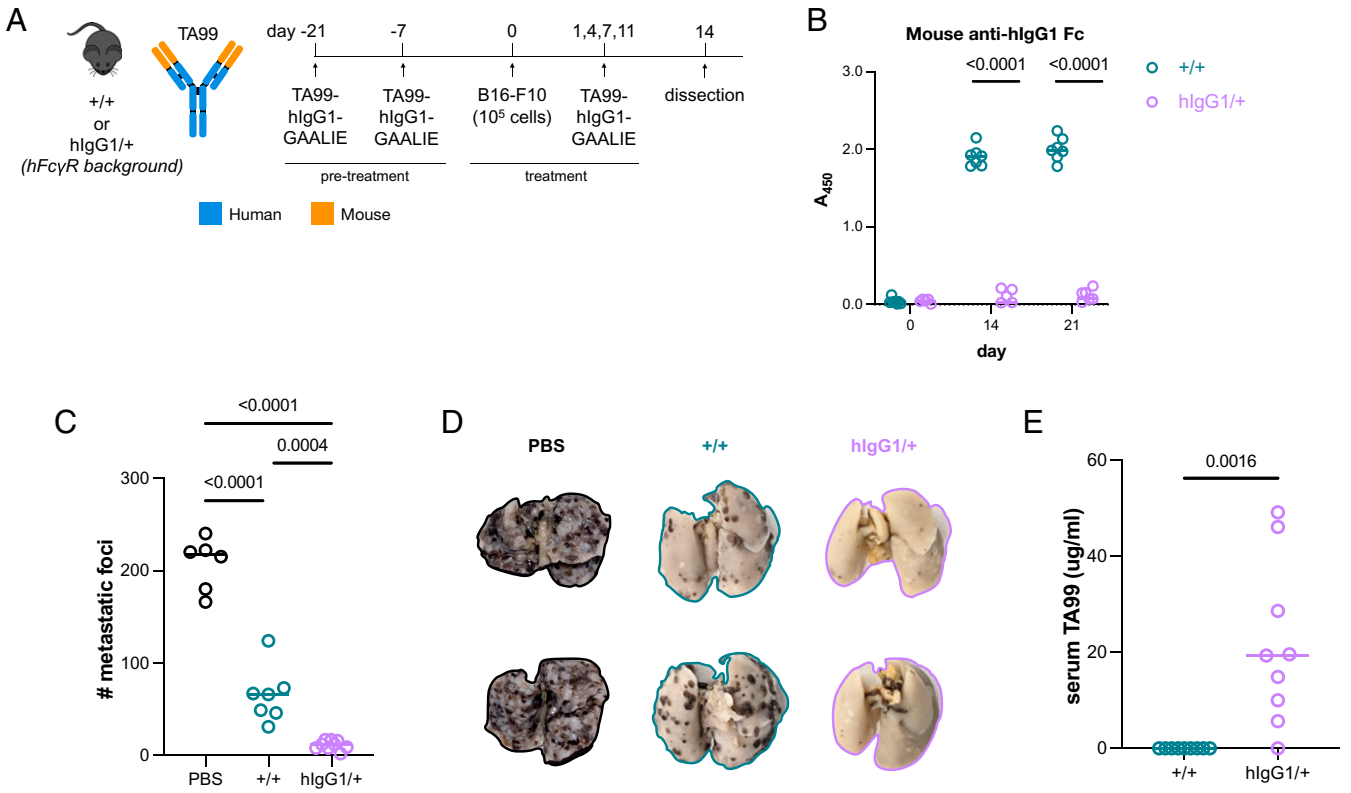

Fig. 5. The hIgG1 knock-in mice show improved clinical outcomes in a B16-F10 melanoma chronic treatment model. (*A*) Pretreatment and treatment schedule of mice subjected to the B16-F10 melanoma metastasis model. Mice were pretreated with TA99-hIgG1 once per week for 3 wk, inoculated intravenously with B16-F10 cells, and treated four times with TA99-hIgG1 at the indicated time points. Mice were killed and their lungs excised on day 14 for analysis. (*B*) Mouse anti-hIgG1 Fc titers were measured by ELISA using hIgG1 Fc for capture and using anti-mouse IgG-HRP for detection. Data are shown as individual biological replicates, with a horizontal line representing the mean (n = 6 to 9 each strain). (*C* and *D*) Lungs were harvested and fixed, and surface lung metastases were counted. Data are shown as individual biological replicates, with a horizontal line representing the mean (n = 6 to 9 each strain). (*E*) Serum was harvested on day 14, and TA99-hIgG1 levels were measured by ELISA using recombinant gp75 for capture and using anti-hIgG-HRP for detection. Quantification was performed by generating a standard curve with purified TA99-hIgG1. Data are shown as individual biological replicates, with a horizontal line representing the mean (n = 6 to 9 each strain).

These fragments were placed within the pBluescript II SK+ cloning vector (Agilent Technologies). In between *IGHG1* Cγ3 and the mouse 3′ homology arm, an *FRT-LoxP-Neo* cassette (w/HindIII adapter into BamHI site of PL451 plasmid) was inserted, resulting in the final construct shown in Fig. 1*A*.

ES Cell Targeting Using CRISPR-Cas9. The transfection of the hIgG1-KI targeting construct utilized the CRISPR-Cas9 system to facilitate efficient HDR while minimizing off-target events. The two guide RNAs, CAGTCCACAGCAATTTCGGC**AGG** and CAAGAACACCGCAACAGTCC**TGG** (PAMs in bold underline), were used to guide the Cas9D10A (nickase), along with the targeting construct, into C57BL/6 ES cells to generate a double-strand break on the mouse Cγ3 domain of *Ighg2c*. The mouse homologous sequences built into the vector ensured replacement with the entire *IGHG1* region represented in the targeting construct. The transfection and subsequent neomycin selection of targeted ES cell clones were performed by the Rockefeller University Gene Targeting Facility.

Due to the increased targeting efficiency of the CRISPR-Cas9 system, a first round of screening ES cell clones by PCR for both the 5′ and 3′ regions of hIgG1 sequence identified positive events that were confirmed by Southern blot analysis of XbaI-digested genomic DNA. A probe that hybridized outside of the targeting vector identified a 3.9-kb band, indicating the presence of a successfully targeted allele, while a 7.0-kb band identified the wild-type *Ighg2c* allele (*SI Appendix*, Fig. S6). Positive clones were selected and microinjected into C57BL/6 mouse blastocysts and implanted into surrogate mice. Pups born were screened for presence of the targeted allele and crossed to mice expressing FLPase for removal of the FRT-flanked Neomycin cassette.

Flow Cytometry. Single-cell suspensions of mouse peripheral blood or splenic cells were obtained, and red blood cells were lysed for 5 min at room temperature, resuspended in PBS containing 0.5% (wt/vol) bovine serum albumin (BSA) and 2 mM (ethylenedinitrilo)tetraacetic acid, and labeled with the following antibodies (all used at 1:200 dilution unless otherwise stated): anti–B220-(clone RA3-6B2)-BrilliantViolet510, anti–NK1.1-(clone PK136)-BrilliantViolet421, anti–Gr-1-(clone RB6-8C5)-BrilliantViolet650, anti–F4/80-BrilliantViolet711, anti–CD3-(clone 17A2), anti–CD11b-(clone M1/70)-PE/Cy7, anti-human FcγRIIa (clone IV.3)-Alexa488 (used at 5 μg·mL^{-1}), anti-human FcγRIIb (clone 2B6)-Dylight650 (used at 5 μg·mL^{-1}), anti-human FcγRIIIa/b (clone 3G8)-PE (used at 5 μg·mL^{-1}), anti-human FcγRI (clone 10.1)-BrilliantViolet605 (used at 5 μg·mL^{-1}), anti–TCRβ-BrilliantViolet711, anti-IgD-FITC, anti-mouse IgG1-APC/Cy7, and anti-human IgG1 (clone M1310G05)-BrilliantViolet421. For FcγR staining, isotype staining was performed with mouse IgG1 isotype control-Dylight650 (used at 5 μg·mL^{-1}), mouse IgG2b kappa isotype control–FITC (used at 5 μg·mL^{-1}), mouse IgG1 kappa isotype control–PE (used at 5 μg·mL^{-1}), and mouse IgG1 kappa isotype control–BrilliantViolet605 (used at 5 μg·mL^{-1}). Data were collected using an Attune NxT flow cytometer (ThermoFisher), and data were analyzed using FlowJo (v10.8) software.

ELISA and T-Dependent and T-Independent Immunizations. Baseline serum IgG levels (Fig. 1) were quantified by ELISA. Diluted sera were added to ELISA plates (Nunc) coated with goat anti-mouse kappa light chain and/or goat anti-mouse lambda light chain antibodies (1 μg·mL^{-1} each, Bethyl Laboratories), and plates were developed with species/isotype-specific horseradish peroxidase (HRP)–conjugated antibodies: goat anti-mouse IgM, goat anti-mouse IgG1, goat anti-mouse IgG2b, goat anti-mouse IgG2c, goat anti-mouse IgG3, or goat anti-human IgG (all from JacksonImmunoResearch). Detection was performed using a TMB Peroxidase Substrate Kit (SeraCare), and reactions were stopped with the addition of 1 M phosphoric acid. Absorbance was measured at 450 nm using a SpectraMax Plus spectrophotometer (Molecular Devices). Background absorbance of negative controls was subtracted from experimental samples, and duplicate wells were then averaged.

Mice were immunized intraperitoneally (i.p.) with TNP-LPS (50 μg; Biosearch Technologies) in 200 μL of PBS or with NP-OVA (50 μg; Biosearch Technologies) in 200 μL of Alum (Thermo Scientific). Some mice were boosted i.p.

with 50 μg of NP-OVA in 200 μL of PBS 21 d after primary immunization. Serum TNP- and NP-specific IgG levels were quantified by ELISA. Sera were diluted and added to ELISA plates coated with TNP-BSA or NP-BSA (Biosearch Technologies), and plates were developed with the same secondary antibodies listed above.

Antibody Engineering and Production. Expi293F cells were used to generate antibodies. Briefly, Expi293F cells were maintained in Expi293 Expression Medium (Thermo Fisher Scientific), and transfected with heavy chain and light chain constructs using an ExpiFectamine 293 Transfection Kit (Thermo Fisher Scientific). The Fc engineering GAALIE variant was generated by site-directed mutagenesis using specific primers, as previously described (18). Five days after transfection, supernatants were collected, centrifuged, and sterile filtered (0.22 μm). Clarified supernatants were incubated with constant agitation with Protein G Sepharose 4 Fast Flow (GE Healthcare) overnight. The next day, Protein G beads were washed with PBS, and bound antibodies were eluted using IgG elution buffer (Thermo Fisher Scientific), dialyzed (molecular weight cutoff 100,000 kDa) in PBS, and sterile filtered again. Purity was assessed by sodium dodecyl sulfate polyacrylamide gel electrophoresis followed by SafeStain blue staining (ThermoFisher), as well as by size exclusion chromatography using a Superdex 200 Increase 10/300GL column (GE Healthcare) on an Äkta Pure 25 HPLC system (data analyzed using Unicorn v.6.3 software).

Tolerance Studies. To study tolerance to hIgG1 antibodies, 100 μg of 3BNC117 (anti-HIV gp120)-hIgG1, 2B8 (anti-CD20)-hIgG1, 2B8-hIgG2, 2B8-hIgG3, or 2B8-hIgG4 were administered i.p. according to the schedule indicated in Fig. 3 *A* and *C*. Serum was harvested at the time points indicated. To detect serum 3BNC117 levels, diluted sera were added to ELISA plates coated with recombinant gp120 (2 $\mu g \cdot mL^{-1}$, Sino Biological), and detected with HRP-conjugated goat anti-human IgG (JacksonImmunoResearch). OD_{450} values were converted to micrograms per milliliter using a standard curve generated with purified 3BNC117. To detect mouse anti-human IgG1 levels, diluted sera were added to plates coated with hIgG1 Fc or an irrelevant mouse chimeric antibody with a mouse IgG1 heavy chain and human kappa light chain (both 2 $\mu g \cdot mL^{-1}$, produced in-house), and detected with HRP-conjugated goat anti-mouse IgG1/2b/2c/3.

Chronic ITP Model. Mice were injected i.v. with 10 μg of anti-glycoprotein IIb antibody (clone 6A6)-hIgG1 on days 0, 1, and 2 of each week for 3 wk. Whole blood was harvested on days 0, 1, 2, and 3 of each week. Platelet counts were measured using an automated hematologic analyzer (Heska HT5). To detect mouse anti-human IgG1 levels, diluted sera were added to plates coated with hIgG1 Fc (2 $\mu g \cdot mL^{-1}$, produced in-house), and detected with HRP-conjugated goat anti-mouse IgG1/2b/2c/3.

Melanoma Chronic Treatment Model. For the B16-F10 lung metastasis model, mice were pretreated i.v. with 40 μg of anti-gp75 (clone TA99)-hIgG1-GAALIE 21 and 7 d before they were injected i.v. with 1×10^5 B16-F10 tumor cells. They received 40 μg of recombinant TA99-hIgG1-GAALIE i.p. on days 1, 4, 7, and 11. On day 14 after tumor challenge, mice were killed, and lungs were analyzed for the presence of surface metastases by counting the number of metastatic foci. To detect mouse anti-human IgG1 levels, diluted sera were added to plates coated with hIgG1 Fc (2 $\mu g \cdot mL^{-1}$, produced in-house), and detected with HRP-conjugated goat anti-mouse IgG1/2b/2c/3. To detect serum TA99-hIgG1-GAALIE levels, diluted sera were added to ELISA plates coated with 5 $\mu g \cdot mL^{-1}$ recombinant gp75 (Creative Biomart), and detected with HRP-conjugated goat anti-human IgG.

Statistics. An unpaired two-tailed *t* test was used when two groups were being compared. One-way ANOVA with Bonferroni's post hoc test was used when more than two groups were compared. GraphPad Prism software (v9.1) was used for all statistical analysis. *P* values of ≤ 0.05 were considered statistically significant (indicated as $*P \leq 0.05$, $**P \leq 0.01$, $***P \leq 0.001$, and $***P \leq 0.0001$).

Data Availability. All study data are included in the article and/or supporting information.

ACKNOWLEDGMENTS. We thank R. Peraza and E. Lam for excellent technical assistance, all the members of the Laboratory of Molecular Genetics and Immunology for helpful discussions, and The Rockefeller University for continued institutional support and its available resources. Research reported in this publication was supported by the National Institute of Allergy and Infectious Diseases (Award U19AI111825 to J.V.R. and S.B.), the National Cancer Institute (Award R35CA196620 to J.V.R. and Award R01CA244327 to S.B.), and by a Medical Scientist Training Program grant from the National Institute of General Medical Sciences (Grant T32GM007739 to the Weill Cornell/Rockefeller/Sloan Kettering Tri-Institutional MD-Ph.D. Program). The content is solely the responsibility of the authors and does not necessarily represent the official views of the NIH.

1. A. Roghanian *et al.*, Antagonistic human FcγRIIB (CD32B) antibodies have anti-tumor activity and overcome resistance to antibody therapy in vivo. *Cancer Cell* **27**, 473–488 (2015).
2. L. Sordé, S. Spindeldreher, E. Palmer, A. Karle, Massive immune response against IVIg interferes with response against other antigens in mice: A new mode of action? *PLoS One* **12**, e0186046 (2017).
3. C. C. Baniel *et al.*, Intratumoral injection reduces toxicity and antibody-mediated neutralization of immunocytokine in a mouse melanoma model. *J. Immunother. Cancer* **8**, e001262 (2020).
4. W. Luo, X. P. Wang, C. E. Kashtan, D. B. Borza, Alport alloantibodies but not Goodpasture autoantibodies induce murine glomerulonephritis: Protection by quinary crosslinks locking cryptic α3(IV) collagen autoepitopes in vivo. *J. Immunol.* **185**, 3520–3528 (2010).
5. C. S. Garris, J. L. Wong, J. V. Ravetch, D. A. Knorr, Dendritic cell targeting with Fc-enhanced CD40 antibody agonists induces durable antitumor immunity in humanized mouse models of bladder cancer. *Sci. Transl. Med.* **13**, eabd1346 (2021).
6. I. Ibarlucea-Benitez, P. Weitzenfeld, P. Smith, J. V. Ravetch, Siglecs-7/9 function as inhibitory immune checkpoints in vivo and can be targeted to enhance therapeutic antitumor immunity. *Proc. Natl. Acad. Sci. U.S.A.* **118**, e2107424118 (2021).
7. P. Weitzenfeld, S. Bournazos, J. V. Ravetch, Antibodies targeting sialyl Lewis A mediate tumor clearance through distinct effector pathways. *J. Clin. Invest.* **129**, 3952–3962 (2019).
8. I. Fulberi, M. Bacher, R. Dodeu, S. Roskam, Evaluating the murine anti-human antibody response and assessment of general activity and cognition after treatment with human intravenous immmunoglobulins in healthy adult C57/B6J mice. *Eur. J. Inflamm.* **12**, 489–497 (2014).
9. P. Smith, D. J. DiLillo, S. Bournazos, F. Li, J. V. Ravetch, Mouse model recapitulating human Fcγ receptor structural and functional diversity. *Proc. Natl. Acad. Sci. U.S.A.* **109**, 6181–6186 (2012).
10. C. Hess *et al.*, T cell-independent B cell activation induces immunosuppressive sialylated IgG antibodies. *J. Clin. Invest.* **123**, 3788–3796 (2013).
11. P. K. Mongini, K. E. Stein, W. E. Paul, T cell regulation of IgG subclass antibody production in response to T-independent antigens. *J. Exp. Med.* **153**, 1–12 (1981).
12. J. F. Scheid *et al.*, HIV-1 antibody 3BNC117 suppresses viral rebound in humans during treatment interruption. *Nature* **535**, 556–560 (2016).
13. F. Nimmerjahn, R. M. Anthony, J. V. Ravetch, Agalactosylated IgG antibodies depend on cellular Fc receptors for in vivo activity. *Proc. Natl. Acad. Sci. U.S.A.* **104**, 8433–8437 (2007).
14. F. Nimmerjahn, J. V. Ravetch, Divergent immunoglobulin g subclass activity through selective Fc receptor binding. *Science* **310**, 1510–1512 (2005).
15. I. Schwab, A. Lux, F. Nimmerjahn, Pathways responsible for human autoantibody and therapeutic intravenous IgG activity in humanized mice. *Cell Rep.* **13**, 610–620 (2015).
16. W. W. Overwijk, N. P. Restifo, B16 as a mouse model for human melanoma. *Curr. Protoc. Immunol.***20**, 20.1.1–20.1.29 (2001).
17. R. Clynes, Y. Takechi, Y. Moroi, A. Houghton, J. V. Ravetch, Fc receptors are required in passive and active immunity to melanoma. *Proc. Natl. Acad. Sci. U.S.A.* **95**, 652–656 (1998).
18. S. Bournazos, D. Corti, H. W. Virgin, J. V. Ravetch, Fc-optimized antibodies elicit CD8 immunity to viral respiratory infection. *Nature* **588**, 485–490 (2020).
19. C. H. Lee *et al.*, An engineered human Fc domain that behaves like a pH-toggle switch for ultra-long circulation persistence. *Nat. Commun.* **10**, 5031 (2019).
20. B. E. Low, G. J. Christianson, E. Lowell, W. Qin, M. V. Wiles, Functional humanization of immunoglobulin heavy constant gamma 1 Fc domain human *FCGRT* transgenic mice. *MAbs* **12**, 1829334 (2020).
21. R. M. Anthony, F. Wermeling, M. C. Karlsson, J. V. Ravetch, Identification of a receptor required for the anti-inflammatory activity of IVIG. *Proc. Natl. Acad. Sci. U.S.A.* **105**, 19571–19578 (2008).
22. R. M. Anthony, T. Kobayashi, F. Wermeling, J. V. Ravetch, Intravenous gammaglobulin suppresses inflammation through a novel T(H)2 pathway. *Nature* **475**, 110–113 (2011).
23. P. Sondermann, A. Pincetic, J. Maamary, K. Lammens, J. V. Ravetch, General mechanism for modulating immunoglobulin effector function. *Proc. Natl. Acad. Sci. U.S.A.* **110**, 9868–9872 (2013).
24. T. T. Wang *et al.*, Anti-HA glycoforms drive B cell affinity selection and determine influenza vaccine efficacy. *Cell* **162**, 160–169 (2015).
25. J. Maamary, T. T. Wang, G. S. Tan, P. Palese, J. V. Ravetch, Increasing the breadth and potency of response to the seasonal influenza virus vaccine by immune complex immunization. *Proc. Natl. Acad. Sci. U.S.A.* **114**, 10172–10177 (2017).